

Analysis on background magnetic field to generate eddy current by pulsed gradient of permanent-magnet MRI

ZU DongLin^{*}, HONG LiMing, CAO XueMing & TANG Xin

Institute of Heavy Ion Physics, Beijing City Key Laboratory of Medical Physics and Engineering, School of Physics, Peking University, Beijing 100871, China

Received October 20, 2009; accepted January 19, 2010; published online March 20, 2010

In this paper the analytical expressions for the magnetic field H and induction B in iron-pole plates generated by MRI gradient coil are given using line-current and the multilayer dielectric plate model with the mirror-image method. Eddy current emanates from the magnetic flux in the iron-pole plates. In order to fully suppress the eddy current, this magnetic flux should be fully eliminated. The research results indicate the magnetic permeability of the resist-eddy plate must be bigger than that of magnetic pole material, i.e. pure iron, and that the resist-eddy plate should be thick enough to be far away from its magnetic saturation.

MRI, suppress eddy current, gradient coil, resist-eddy plate, mirror-image method

Citation: Zu D L, Hong L M, Cao X M, et al. Analysis on background magnetic field to generate eddy current by pulsed gradient of permanent-magnet MRI. Sci China Tech Sci, 2010, 53: 886–891, doi: 10.1007/s11431-010-0120-6

In MRI, three linear, orthogonal, pulsed magnetic field-gradients are used not only for spatial encoding of the NMR signal but also to generate gradient echoes (GE), resulting in GE sequences, EPI sequence, etc. Furthermore, the pulsed gradient is also used for diffusion-weighted imaging, diffusion-tensor imaging, destroying phase coherence and compensating for flow [1], etc. However, there is some annoying side-effect for the pulsed gradient. It would generate an eddy-current in the metallic material near the gradient coil, especially in the iron-pole plates. The magnetic field generated by the eddy current overlaps with the original gradient magnetic field, resulting in a breach of the canonical conjugate relationship between wave number and space, thus eddy artifact and distortions.

Engineers have excogitated many methods to overcome the artifact and distortions induced by the eddy-current. The widely used way is “temporal eddy-current compensation”

[2, 3], i.e. gradient waveform preemphasis. The idea underlying waveform preemphasis is to intentionally distort the current waveform that is input to the gradient coil, such that the preemphasis distortion cancels the subsequent eddy-current distortion. The time dependence of eddy-currents is accurately modeled by an exponential function [4]. Using this model, eddy currents are characterized by a few time constants and coefficients that are called amplitudes. The time constants describe the rate of exponential buildup and decay after a gradient change. The time constants and coefficients depend on the magnet geometry and sequence. Accurate preemphasis requires a quantitative model of eddy currents. Hence the effect of this method is limited. The way to suppress thoroughly eddy-current is called “eddy-current shielded by itself”. The basic idea is not allowing the gradient flux to enter into the metal materials nearby.

The method of shielding eddy-current by itself is divided into two classes of passive shielding [5] and active shielding [6–9]. In a superconducting (SC) MRI system, wire of gradient coil is limited on a cylindrical surface [10–13]. Passive

*Corresponding author (email: dlzu@pku.edu.cn)

shielding is implemented through outside the gradient coils to apply a metallic cylinder with a certain thickness and a radius larger than that of the gradient coil. The principle is making use of the magnetic flux generated by the eddy-current (with an opposite flow direction of the current in the main gradient coils) which is induced by the gradient field in the inner wall of the metallic cylinder (skin effect) to cancel the magnetic flux outside the metallic cylinder. A fatal problem of this method is that the phase of the eddy-current has an extra lag (due to $\nabla \times \vec{E} = -\partial \vec{B} / \partial t$), so it can not cancel accurately the main gradient field flux. Besides, because the spectrum of the pulse gradient is located between 0 Hz and 10 kHz [14, 15], the shielding cylinder can't block those magnetic fluxes with low frequencies. Therefore the passive shielding method is not used anymore. Active shielding uses both main gradient coils and shielding coils. It is designed as a whole one using target-field method, its current phase is opposite strictly, so the gradient field flux outside the gradient coil is canceled completely. Therefore, there is no flux leaking into the metal pieces nearby, especially the iron-pole plates. Thus the eddy-current problem is solved downright. This is a prerequisite of operating EPI sequence in the clinical SC MRI. In a permanent-magnet MRI system, the active shielding gradient coils can certainly be used. However, a higher cost is needed to pay. Because of the current flow direction in the shielding coil is opposite to that in the main gradient coil by and large, when they cancel the magnetic flux outside the gradient coil, the useful gradient over the imaging volume is reduced too. In order to minish the side effect as much as possible the distance between the shielding coil and the main gradient coil must be kept big enough. Otherwise, the useful gradient over the imaging volume will be reduced so much that a larger power gradient amplifier with larger current output must be used. Consequently, it results in a larger thermal load, so that a cooling system using flowing water has to be added.

A big distance between the shielding coil and the main gradient coil undoubtedly requires to increase the distance between N pole and S pole of the magnet. It consequently increases the manufacture cost of the magnet. So the third method of suppressing eddy-current emerged. A layer of material with high magnetic permeability and high resistivity, called "resist-eddy plate", is added between the gradient coil and the iron magnetic pole instead of adding a shielding coil. This kind of material may be silicon steel sheets, nm-crystal strap-material or non-crystal strap-material. These materials have an ability of collecting magnetic flux. Making use of this kind of material would achieve the magnetic flux to be compressed and reduce significantly magnetic flux leaked into the iron magnetic pole. The effect depends on the thickness and the magnetic permeability of the resist-eddy plate. The aim of suppressing eddy-current could be achieved no other than under a reasonable design condition.

The following case often happens: after the eddy-current problem seems to be solved, it recurs as soon as we operate with a faster pulse sequence to raise the imaging speed. So the problem of eddy-current in MRI is a topic needed to be researched on and on. The aim of this article utilizes an ideal model for some quantitative calculation to set up a correct concept basis of fully suppressing eddy-current.

1 Mirror-image method of magnetostatics

In an unbounded vacuum, the magnetic field induced by a current flow can be calculated with the Biot-Savart formula. Yet, we must consider the influence of the magnetization current if there is ferromagnetic medium nearby. In a permanent-magnet MRI system, the coil current-carrying is in the vicinity of the iron magnetic pole surface. The tropism of the current flow is parallel to the magnetic pole surface. We use an ideal model to calculate the magnetic field of a rectilinear current. There would not be eddy-current if only the magnetic field does not sink into the iron magnetic pole.

For a universal discussion, we suppose that the half space above the reference interface is filled with magnetic medium 1 which has a relative permeability μ_1 , while another half space below the reference interface is filled with magnetic medium 2 which has a relative permeability μ_2 . An infinitely long straight wire carrying current I in the above half space parallels to the interface and leaves the interface with a distance of d . How to obtain the magnetic field H and the induction B everywhere in this situation? The media are magnetized in the magnetic field induced by the current I . There appears a distribution of magnetizing-current in both medium 1 and medium 2. The magnetizing-current also induces a magnetic field. Arriving at a steady state the magnetizing-current will have a determinate distribution. Note that the distributions of the magnetizing-currents in two kinds of media are different and complicated. We can simulate the magnetizing-currents using some mirror image currents.

The coordinates are shown as in Figure 1. According to the principle of the mirror-image method of magnetostatics [16, 17], when calculating the magnetic field in the above half space, we suppose that both above and below half spaces are filled with magnetic medium 1 described by permeability $\mu_1\mu_0$ (μ_0 is the vaccum-permeability) and the mirror-image, I' , must be located outside the above half space, i.e. in the below half spaces. Thus, this magnetic field is produced together by the original current I and the mirror image current I' as shown in Figure 1(a).

By the same principle when calculating the magnetic field in the below half space, we suppose that both the above and below half spaces are filled with magnetic medium 2 described by permeability $\mu_2\mu_0$. The magnetic field is produced by mirror current I'' , I'' is at the same place as the original current I , as shown in Figure 1(b) [16, 17]. The

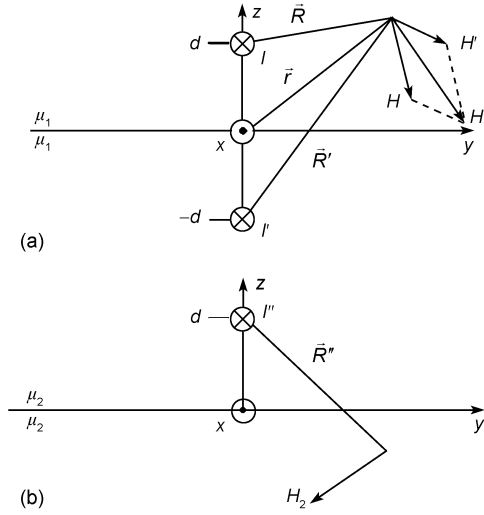


Figure 1 The model of two-layer media.

flow directions of I' and I'' are the same as I . Making use of the Ampere loop theorem in medium, we can obtain the magnetic field strengths on both sides with respect to the interface easily. Then making use of the boundary conditions on \vec{H} and \vec{B} , i.e., $H_{2t} = H_{1t}$ and $B_{2n} = B_{1n}$ (Subscripts t and n represent the tangential and normal tropism, respectively), we can get the mirror currents:

$$\begin{cases} I' = \frac{\mu_2 - \mu_1}{\mu_2 + \mu_1} I, \\ I'' = \frac{2\mu_1}{\mu_2 + \mu_1} I. \end{cases} \quad (1)$$

Thus, we obtain the magnetic fields of the above and below half spaces respectively:

$$\vec{H}_1 = \frac{I}{2\pi} \left[\frac{(z-d)\vec{e}_y - y\vec{e}_z}{y^2 + (z-d)^2} + \frac{\mu_2 - \mu_1}{\mu_2 + \mu_1} \frac{(z+d)\vec{e}_y - y\vec{e}_z}{y^2 + (z+d)^2} \right] \quad (z>0), \quad (2)$$

$$\vec{H}_2 = \frac{\mu_1 I}{\pi(\mu_2 + \mu_1)} \cdot \frac{(z-d)\vec{e}_y - y\vec{e}_z}{y^2 + (z-d)^2} \quad (z<0). \quad (3)$$

2 The situation of air and pure-iron magnetic pole

Suppose that the above half space is air and the below half space is pure-iron, i.e., $\mu_1=1$ and $\mu_2=\mu_r$, where μ_r is the relative permeability of iron. Putting all this into eq. (2) we obtain the magnetic field and the magnetic induction in the above half space:

$$\vec{H}_1 = \frac{I}{2\pi} \left[\frac{(z-d)\vec{e}_y - y\vec{e}_z}{y^2 + (z-d)^2} + \frac{\mu_r - 1}{\mu_r + 1} \cdot \frac{(z+d)\vec{e}_y - y\vec{e}_z}{y^2 + (z+d)^2} \right] \quad (z>0), \quad (4a)$$

$$\vec{B}_1 = \frac{\mu_0 I}{2\pi} \left[\frac{(z-d)\vec{e}_y - y\vec{e}_z}{y^2 + (z-d)^2} + \frac{\mu_r - 1}{\mu_r + 1} \cdot \frac{(z+d)\vec{e}_y - y\vec{e}_z}{y^2 + (z+d)^2} \right] \quad (z>0). \quad (4b)$$

The magnetic field in the above half space has a second item because of iron in the below half space. If μ_r is very large, then $(\mu_r - 1)/(\mu_r + 1) \approx 1$, so the magnetic field near the interface is twice as big as that without iron in the below half space. Actually, the μ_r of the iron magnetic pole at its work point may not be very large. The field in iron of the below half space is as follows:

$$\vec{H}_2 = \frac{2I}{2\pi(\mu_r + 1)} \cdot \frac{(z-d)\vec{e}_y - y\vec{e}_z}{y^2 + (z-d)^2} \quad (z<0), \quad (5a)$$

$$\vec{B}_2 = \frac{2\mu_0\mu_r I}{2\pi(\mu_r + 1)} \cdot \frac{(z-d)\vec{e}_y - y\vec{e}_z}{y^2 + (z-d)^2} \quad (z<0). \quad (5b)$$

In the iron-pole plate, \vec{H}_2 is reduced, because of polarization, a demagnetizing field is induced in the medium. Meanwhile if μ_r is very large, \vec{B}_2 increases to approximately twice as large as that in air. This is a result of supposing medium 2 (μ_2) with an infinite big thickness. If the surface of the magnetic pole plate has a complex shape, the mirror-image method may be not exact. For a flat-surface pole plate, even if you can calculate the field gradient exactly produced by a gradient coil using the mirror-image method, the eddy-current still has a big influence on the medical imaging, because the pulse gradient is a function of time. If replacing media μ_2 by a resist-eddy plate, then that is what we will discuss later.

3 Gradient coil and resist-eddy material

Though the largest relative permeability μ_r of the materials like pure iron and silicon steel sheets used for electric engineering can be as high as 10000 or above. The largest μ_r of the iron-based nm-crystal material achieves 500000, and the largest μ_r of iron-based non-crystal material achieves 200000. But their hysteresis loop as shown in Figure 2 is a result measured in the situation without demagnetizing-field. It is far away from the ideal situation under the MRI-magnet application condition, and their effective permeabilities μ_r 's are much lower. The iron magnetic pole and resist-eddy plate are nearly in the same background magnetic field larger than the work magnetic field B_0 of the imaging region, so these passive magnetic media have an work point close to their saturated point. If the resist-eddy plate is very thin, approaching saturation magnetization, then its valid μ_r may be very small. If $\mu_r=10$, according to eq. (4a), on the surface of the resist-eddy plate ($z=0_+$), the y-component of the field (absolute value), i.e. the tangential component

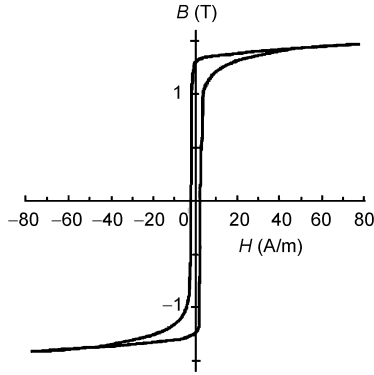


Figure 2 The hysteresis loop of a non-crystal based-on-iron material.

$$H_{1,t} = \frac{I}{11\pi} \cdot \frac{d}{y^2 + d^2}. \quad (6a)$$

It is clearly smaller than $H_{01,t} = \frac{I}{2\pi} \cdot \frac{d}{y^2 + d^2}$, which is

obtained without resist-eddy plate. The z - component of the field (absolute value) i.e. the normal component

$$H_{1,n} = \frac{10I}{11\pi} \cdot \frac{y}{y^2 + d^2} \quad (6b)$$

It is larger than $H_{01,n} = \frac{I}{2\pi} \frac{y}{y^2 + d^2}$, which is obtained

without resist-eddy plate. Because the gradient field is in a normal direction, it can be enhanced. Now viewing in the resist-eddy material (remember we suppose its $\mu_r=10$), we have the magnetic induction as

$$\vec{B}_2 = \frac{10\mu_0 I}{11\pi} \cdot \frac{(z-d)\vec{e}_y - y\vec{e}_z}{y^2 + (z-d)^2}. \quad (7)$$

The absolute value is larger than $\bar{B}_2 = \frac{\mu_0 I}{2\pi} \cdot \frac{(z-d)\vec{e}_y - y\vec{e}_z}{y^2 + (z-d)^2}$,

which is obtained without resist-eddy plate ($\mu_r=1$). The utmost value is double the latter. So we know that within resist-eddy plate, the magnetic induction line does not become dense suddenly since the boundary condition on the interface must be satisfied. Under the best condition, the B in the resist-eddy plate will double. Consequently, the gradient strength in the air will double too. We can conclude that whatever material is added, the eddy-current will reduce and the gradient will enhance. The inductance of the gradient coil will certainly increase.

From eq. (7), the normal component and the tangential component of the B field are increased evenly. This is a result from supposing resist-eddy plate has an infinite big thickness. Actually, the thickness of the resist-eddy plate is finite, we need to calculate multi-order mirror images. So, the thickness of the resist-eddy plate and the valid μ_r

at its work point are two key parameters. The model with two kinds of materials is not enough to illuminate the problem. Therefore we discuss the model with three kinds of materials.

4 Model with three kinds of materials

A model with three kinds of materials is shown in Figure 3. The distance between the current I and the first reference interface is a (see Figure 3). We suppose the thickness of the second layer of medium (μ_2) is d (see Figure 3), while the thickness of medium 1 (μ_1) and medium 3 (μ_3) still are half-infinite big. We can obtain the magnetic field in these three areas with the mirror-image method. Take the coordinates as shown in Figure 4. The localities of the mirror-image currents in the first area are shown in Figure 4(a), and those of the second and third areas in Figures 4(b) and (c), respectively. We suppose the reflection coefficients

$$\begin{cases} k_1 = \frac{\mu_1 - \mu_2}{\mu_1 + \mu_2}, \\ k_2 = \frac{\mu_3 - \mu_2}{\mu_3 + \mu_2}. \end{cases} \quad (8)$$

So the mirror-image currents in the three areas are as below.

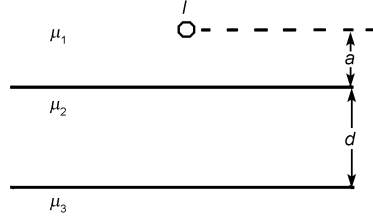


Figure 3 Three-medium model for calculation.

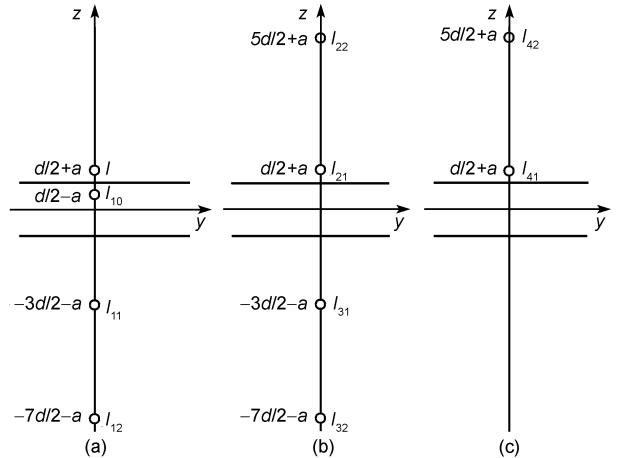


Figure 4 Positions of the mirror-image currents. (a) μ_1 region; (b) μ_2 region; (c) μ_3 region.

1) Area 1 (μ_1).

$$\begin{cases} z_{10} = \frac{d}{2} - a, \\ I_{10} = -k_1 I, \\ z_{1n} = \frac{d}{2} - a - 2nd, \\ I_{1n} = (k_1 k_2)^n \frac{(1-k_1)(1+k_1)}{k_1} I, \end{cases} \quad (n=1, 2, \dots). \quad (9a)$$

2) Area 2 (μ_2).

$$\begin{cases} z_{2n} = -\frac{3d}{2} + a + 2nd, \\ I_{2n} = (k_1 k_2)^n \frac{1+k_1}{k_1 k_2} I, \\ z_{3n} = \frac{d}{2} - a - 2nd, \\ I_{3n} = (k_1 k_2)^n \frac{1+k_1}{k_1} I, \end{cases} \quad (n=1, 2, \dots). \quad (9b)$$

3) Area 3 (μ_3).

$$\begin{cases} I_{4n} = (k_1 k_2)^n \frac{(1-k_2)(1+k_1)}{k_1 k_2} I, \\ z_{4n} = -\frac{3d}{2} + a + 2nd, \end{cases} \quad (n=1, 2, \dots). \quad (9c)$$

The magnetic field strengths in the three areas are as follows.

1) Area 1 (μ_1).

$$\vec{H}_1 = \frac{I}{2\pi} \left[\frac{z - \left(\frac{d}{2} + a \right)}{\left[z - \left(\frac{d}{2} + a \right) \right]^2 + y^2} \vec{e}_y - \frac{-k_1 I}{\left[z - \left(\frac{d}{2} + a \right) \right]^2 + y^2} \vec{e}_z \right] + \frac{-k_1 I}{2\pi} \left[\frac{z - \left(\frac{d}{2} - a \right)}{\left[z - \left(\frac{d}{2} - a \right) \right]^2 + y^2} \vec{e}_y - \frac{y\vec{e}_z}{\left[z - \left(\frac{d}{2} - a \right) \right]^2 + y^2} \right] + \sum_{n=1}^{\infty} \frac{(k_1 k_2)^{n-1} (1-k_1^2) k_2 I}{2\pi} \times \left[\frac{z - \left(\frac{d}{2} - a - 2nd \right)}{\left[z - \left(\frac{d}{2} - a - 2nd \right) \right]^2 + y^2} \vec{e}_y - \frac{y\vec{e}_z}{\left[z - \left(\frac{d}{2} - a - 2nd \right) \right]^2 + y^2} \right] \quad (n=1, 2, \dots). \quad (10a)$$

2) Area 2 (μ_2).

$$\vec{H}_2 = \sum_{n=1}^{\infty} \frac{(k_1 k_2)^{n-1} (1+k_1) I}{2\pi} \times \left[\frac{z - \left(-\frac{3d}{2} + a + 2nd \right)}{\left[z - \left(-\frac{3d}{2} + a + 2nd \right) \right]^2 + y^2} \vec{e}_y - \frac{y\vec{e}_z}{\left[z - \left(-\frac{3d}{2} + a + 2nd \right) \right]^2 + y^2} \right] + \sum_{n=1}^{\infty} \frac{(k_1 k_2)^{n-1} (1+k_1) k_2 I}{2\pi} \times \left[\frac{z - \left(\frac{d}{2} - a - 2nd \right)}{\left[z - \left(\frac{d}{2} - a - 2nd \right) \right]^2 + y^2} \vec{e}_y - \frac{y\vec{e}_z}{\left[z - \left(\frac{d}{2} - a - 2nd \right) \right]^2 + y^2} \right] \quad (n=1, 2, \dots). \quad (10b)$$

3) Area 3 (μ_3).

$$\vec{H}_3 = \sum_{n=1}^{\infty} \frac{(k_1 k_2)^{n-1} (1+k_1) (1-k_2) I}{2\pi} \times \frac{[z - (-3d/2 + a + 2nd)] \vec{e}_y - y \vec{e}_z}{[z - (-3d/2 + a + 2nd)]^2 + y^2}. \quad (10c)$$

We plot the magnetic induction in the three areas according to $\vec{B}_i = \mu_i \vec{H}_i$. Because $\nabla \cdot \vec{B} = 0$, it is convenient to plot the B lines making use of stream function method.

If we let $\mu_3 = \mu_2$, then $k_2 = 0$, so that a result of single transmission surface is obtained, which is consistent perfectly with the results expressed by eqs. (2) and (3). Suppose $a/d = 0.3$, keep 100 mirror-image currents, 28 magnetic inductance lines. For the three layers of media, we consider 6 cases, and the results calculated are shown in Figure 5. Figure 5(a) shows an anticipated result for the case that three areas all are air. Figures 5(b)–(d) show the results for the cases that the middle area is a resist-eddy plate with valid $\mu_r = 10, 100$ and 1000, respectively, while both the side areas of the resist-eddy plate are air. These results demonstrate that the higher the valid μ_r , the better the effect of suppressing eddy-current. The actual application situation is that one side of the resist-eddy plate is iron magnetic pole while another side is air. Figure 5(e) shows when the μ_r of the resist-eddy plate is one order of magnitude larger than that of the iron magnetic pole, the effect of suppressing eddy-current is better. While Figure 5(f) shows an opposite situation. When the μ_r of the resist-eddy plate is one order of magnitude smaller than that of the iron magnetic pole, the effect of suppressing eddy-current is poor. It should be emphasized that what is shown in Figure 5 is the zero-frequency component of the gradient magnetic flux. For the alternate components of the gradient magnetic flux, in the iron magnetic pole, the eddy-current and magnetic induction lines will concentrate towards its surface due to the skin effect. Inside the resist-eddy plate there is no significant skin effect due to its high resistivity or layer-stacked structure to cut off the eddy-current paths. The zero-frequency component of the gradient magnetic flux is the very background field inducing eddy-current.

5 Discussion and conclusions

It is always effective to compress the magnetic flux, reduce the eddy-current, enhance the gradient strength if a resist-eddy plate is used. However, to suppress the eddy-current fully, some quantitative relationship should be known. For the resist-eddy plate we should choose a material which has a higher relative permeability μ_r than that of the pure iron. Various silicon steel sheets produced by different companies all over the world have different relative perme-

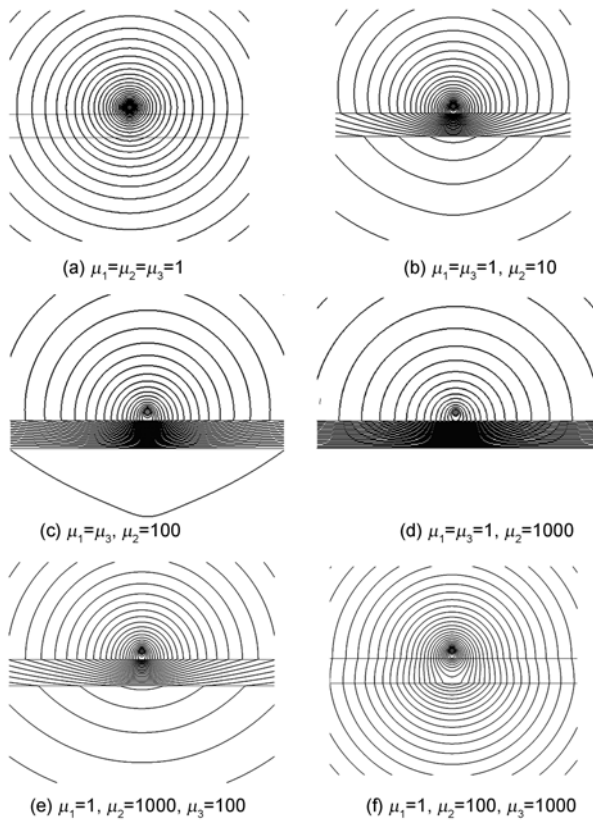


Figure 5 The results calculated for three-layer-medium model corresponding to various cases (Plotting parameters used: $a/d=0.3$; 100 mirror-image currents, 28 magnetic induction lines).

abilities (μ_r), we must carefully filtrate them. The nm-crystal or non-crystal tape-material should be preferred, while any ferromagnetic is not trusted. Moreover, the resist-eddy plate should be thick enough, otherwise its valid μ_r becomes low. Because the valid μ_r of a material will reduce enormously when approaching saturation. We should know clearly what positions of the hysteresis loop the work points of the iron magnetic poles and the resist-eddy plates locate at, and the variation range of the work points moving up and down at the second quadrant of its hysteresis loop when the gradient varies between the positive and negative limits.

With the method of resist-eddy plate, different schemes

may result in different effects because the quantitative relationship discussed above is satisfied or not. Some foreign MRI company has nicely resolved the problem of eddy-current artifact. In addition it is necessary to point out that simply interposition of a resist-eddy plate would influence the uniformity and the strength of the main magnetic field B_0 designed originally. Therefore, we should consider it as a whole when designing an MRI permanent magnet.

This work was supported by the National Natural Science Foundation of China (Grant No. 60871001).

- 1 Zu D L. Magnetic Resonance Imaging (in Chinese). Beijing: Higher Education Press, 2004
- 2 Morich M A, Lampman D A, Dannels W R, et al. Exact temporal eddy current compensation in magnetic resonance imaging systems. *IEEE T Med Imag*, 1988, 7(3): 247–254
- 3 van Vaals J J, Bergman A H. Optimization of eddy-current compensation. *J Magn Reson*, 1990, 90: 52–70
- 4 Bernstein M, King K, Zhou X H. Handbook of MRI Pulse Sequence. New York: Elsevier Press, 2004
- 5 Turner R, Bowley R M. Passive screening of switched magnetic field gradients. *J Phys E* 1986, 19: 876–979
- 6 Turner R. A target field approach to optimal coil design. *J Phys D: Appl Phys*, 1986, 19: L147–L151
- 7 Mansfield P, Chapman B. Active magnetic screening of gradient coils in NMR imaging. *J Magn Reson*, 1986, 66: 573–576
- 8 Bowtell R, Mansfield P. Screened coil designs for NMR imaging in magnets with transverse field geometry. *Meas Sci Technol*, 1990, 1: 431–439
- 9 Liu W T, Zu D L, Tang X, et al. Target-field method for MRI biplanar gradient coil design. *J Phys D: Appl Phys*, 2007, 40: 4418–4424
- 10 Carlson J W, Derby K A, Hawrysko K C, et al. Design and evaluation of shielded gradient coils. *Magn Reson Med*, 1992, 26: 191–206
- 11 Turner R. Gradient coil design: A review of methods. *Magn Reson Imag*, 1993, 11: 903–920
- 12 Turner R. Electrical coils. US Patent, 5, 289, 151, 1994-02-22
- 13 Tang X, Zu D, Bao S. A new design method for asymmetrical head gradient coils used for superconducting MRI scanner. *Prog Nat Sci*, 2004, 14(9): 753–757
- 14 Wang W, Eisenberg S R. A three-dimensional finite element method for computing magnetically induced currents in tissues. *IEEE T Mag* 1994, 30: 5015–5023
- 15 Bowtell R, Bowley R M. Analytic calculations of the E -fields induced by time-varying magnetic field generated by cylindrical gradient coils. *Magn Reson Med*, 2000, 44: 782–790
- 16 Wang Q, Li D G, Gong K. Electromagnetic Field Theory Ground-work (in Chinese). Beijing: Tsinghua University Press, 2001
- 17 Zu D L. Electrodynamics (in Chinese). Beijing: Tsinghua University Press, 2006